

<sup>8</sup>Although the shape of the angular distribution was measured with 10.1-MeV tritons, the magnitude of the cross section was measured with 12-MeV tritons. Estimates with our zero-range code indicate that the effect of this 2-MeV energy difference on the magnitude

of the cross section should be less than 7%.

<sup>9</sup>B. F. Bayman and A. Kallio, Phys. Rev. **156**, 1121 (1967).

<sup>10</sup>F. D. Becchetti, Jr., and G. W. Greenlees, Phys. Rev. **182**, 1190 (1969).

## Formation of Geons and Black Holes

Ulrich H. Gerlach\*

*Battelle Memorial Institute, Columbus, Ohio 43201*

(Received 21 September 1970)

We determine the dynamics of a spherically symmetric, thin-shelled ensemble of collisionless particles. All the stable and unstable equilibrium configurations (which we find to be stable against single-particle decay) are classified with the help of a variational principle. Applying this principle to zero-rest-mass particles (e.g., gravitational geon), we find that quantum geometrodynamics must be applied when the geon has low angular momentum and is in its ground state.

The hydrodynamics of spherically symmetric gravitational collapse<sup>1</sup> has advanced to the stage where, in order to gain new knowledge, one must merely solve the appropriate equations for the particular situation under study. Because of their nonlinearity, some very interesting information can be extracted from these equations only with great financial efforts: Involved computer calculations are necessary to solve the equations.<sup>2</sup>

Consequently, our work has been to set up and solve analytically an archetypical model for gravitational collapse<sup>3,4</sup>: Although this model ignores the detailed internal, hydrodynamic features, it incorporates those essential features that determine whether or not a black hole or a geon is formed. Consider a spherically symmetric ensemble of noncolliding particles (with or without rest mass), each having a given angular momentum  $l$ . The stress-energy tensor and the particle flux vector are<sup>5</sup>

$$T_{\nu}^{\mu} = \int N p_{\nu} p^{\mu} d\omega,$$

$$J^{\mu} = \int N p^{\mu} d\omega,$$

respectively. Here  $N$  is the invariant single-particle distribution function that satisfies the Liouville equation,  $p^{\mu}$  is the particle four-momentum, and  $d\omega$  is the invariant three-momentum volume element.

We shall selectively focus on ensembles that are hollow thin-shelled spheres. Within a shell the particles are churning back and forth within a small energy range. Consequently, an observer moving with the thin shell notices that

$$T_0^0 = c p_0 J^0, \quad (1)$$

where  $c$  is the speed of light.

First we wish to determine the equilibrium configurations of the particle ensemble. Consequently, we focus attention on all the momentarily static configurations. The conservation of particle number and the initial-value equations of general relativity yield

$$da/dR = 4\pi R^2 J^0 \exp\left[\frac{1}{2}(\lambda + \nu)\right] \quad (2)$$

and

$$dm/dR = -4\pi R^2 T_0^0 \quad (3)$$

in the Schwarzschild coordinates,

$$ds^2 = -e^{\nu} dt^2 + e^{\lambda} dR^2 (d\theta^2 + \sin^2\theta d\varphi^2). \quad (4)$$

Here  $a$  and  $m$  are the particle number and the mass enclosed by a sphere of radius  $R$ . The radial metric coefficient is given by<sup>6</sup>

$$e^{\lambda} = (1 - 2m^*/R)^{-1},$$

and the energy of the particles is peaked around

$$-c p_0 e^{-\nu/2} = c(l^2/R^2 + \mu^2 c^2)^{1/2}, \quad (5)$$

where  $l$  is the conserved angular momentum and  $\mu$  is the rest mass of each particle. For momentarily static particle ensembles, having total particle number  $A$ , the total mass energy as seen by a distant observer is determined from the differential equation

$$\frac{dm^*}{da} = \left(1 - \frac{2m^*}{R}\right)^{1/2} \left(\frac{l^2}{R^2} + \mu^2 c^2\right)^{1/2} \frac{G}{c^3}. \quad (6)$$

This equation is the consequence of dividing Eq. (2) into Eq. (3) and then making the appropriate substitutions for  $e^{\lambda/2}$ ,  $T_0^0$ , and  $p_0 e^{-\nu/2}$ . Integrat-

ing Eq. (6) over  $m^*$  from 0 to  $M_\infty^*$  and  $a$  from 0 to  $A$  yields

$$M_\infty c^2 = Ac \left( \frac{l^2}{R^2} + \mu^2 c^2 \right)^{1/2} - \frac{1}{2} \frac{A^2 c^2}{R} \left( \frac{l^2}{R^2} + \mu^2 c^2 \right) \frac{G}{c^4} \quad (7)$$

for the total observed mass energy. It can also be directly obtained from a quasi-Newtonian argument: Equation (7) is the sum of (a) the total (rest mass and kinetic energy) mean energy of  $A$  particles as given by the fourth physical component of  $p_\mu$  in Eq. (5), and (b) the Newtonian gravitational energy due to  $A$  particles making up a hollow sphere:

$$- \frac{1}{2} \frac{(\text{mass})^2 G}{R} = - \frac{1}{2} \left[ A \frac{1}{c} \left( \frac{l^2}{R^2} + \mu^2 c^2 \right)^{1/2} \right]^2 \frac{G}{R}.$$

It is evident that not only the rest mass but also the kinetic energy makes a decisive contribution to the gravitational energy.

Figure 1 gives the total observed mass energy of a material particle ensemble as a function of the radius for various angular momenta.

To select the equilibrium configurations one must focus one's attention on those configurations that extremize  $M_\infty$  with respect to configurations which have the same total particle num-

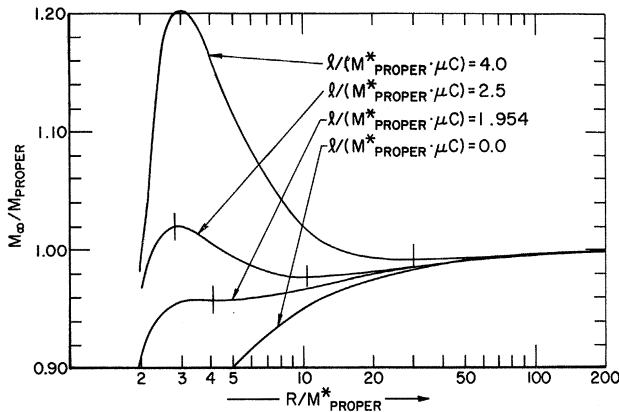


FIG. 1. "Effective potential" for collective motion of material particles. The ordinate measures  $M_\infty$ , Eq. (7), the mass seen by a distant observer, in units  $M_{\text{prop}} = A\mu c^2$ . The abscissa measures the radial coordinate  $R$  of the thin shell in geometric mass units  $M^*$ . The curves represent the locus of momentarily static configurations for various angular momenta measured in units  $M_{\text{prop}}^* \mu c$ . In these units the curves, Eq. (7), are  $y = (1 + L^2/X^2)^{1/2} - \frac{1}{2}(1 + L^2/X^2)/X$ . Observe that although there do exist stable and unstable equilibrium configurations for sufficiently high angular momenta  $l$ , below  $l_{\text{crit}}/M_{\text{prop}}^* \mu c = 1.954$  there exists no equilibrium configuration whatsoever.

ber  $A$ , but whose radii differ slightly.<sup>7</sup> Figure 1 makes apparent not only which configurations are in equilibrium but also which are stable and which are unstable with respect to collective motion. A catalog of both the stable and unstable configurations as characterized by the angular momentum and the radius of the collective ensemble is given in Fig. 2.

Are the equilibrium configurations stable with respect to single-particle evaporation? Yes! A simple examination of the single-particle potential in relation to the catalog of equilibrium configurations shows that the single-particle potential always has a minimum precisely at the position of the shell—a minimum that is sharper the thinner the shell is.

The dynamics of collapsing particle ensembles we obtain directly by solving the Einstein field equations in comoving coordinates<sup>8</sup>:

$$ds^2 = -e^{2\phi} dt^2 + e^\lambda dr^2 + R^2(r, t)(d\theta^2 + \sin^2\theta d\varphi^2). \quad (8)$$

More simply, however, we write down particle and mass conservation, Eqs. (1) and (2), in comoving coordinates:

$$da/dr = 4\pi R^2 J^0 e^{\lambda/2 + \phi} \quad (2')$$

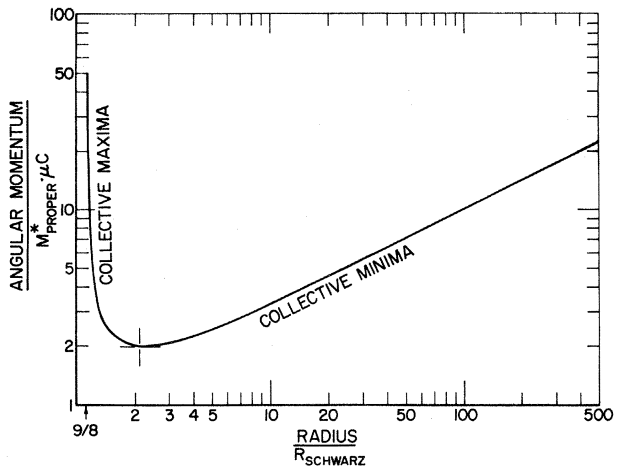


FIG. 2. Catalog of the collective equilibrium configurations. The ordinate measures the angular momentum of each particle in a configuration in units  $M_{\text{prop}}^* \mu c = A\mu c^2 \mu c$ . The abscissa measures the radius in units of Schwarzschild radii ( $R_{\text{Schwarz}} = 2M_\infty^*$ ) of a configuration. Thus, the lower unbroken curve depicts both the unstable and the stable collective equilibrium configurations. It is to be noted that below  $l_{\text{crit}} = 1.954 M_{\text{prop}}^* \mu c$ , where  $R = 2.1323 (2M_\infty^*)$ , there exists no equilibrium configuration. Also note that as  $l \rightarrow \infty$ , the unstable branch approaches the dimension of a geon,  $R = (9/8) (2M_\infty^*)$ .

and

$$dm/dr = -4\pi R^2 T_0^0 \partial R / \partial r. \quad (3')$$

Then transform the metric from the Schwarzschild coordinates, Eq. (4), to comoving coordinates, Eq. (8), and introduce the rate of change of  $R$  with respect to proper comoving time,  $U \equiv e^{-\varphi} \partial R / \partial t$ , and thus obtain

$$e^{-\varphi} = \frac{1 - 2M^*/R}{(1 + U^2 - 2M^*/R)^{1/2}},$$

$$e^{-\lambda/2} \partial R / \partial r = (1 + U^2 - 2M^*/R)^{1/2}. \quad (9)$$

In the comoving frame the mean energy of the particles is

$$-c p_0 e^{-\varphi/2} = c(l^2/R^2 + \mu^2 c^2)^{1/2}, \quad (5')$$

Eq. (3), on the other hand, does not change its form. With these observations we again obtain a differential equation similar to Eq. (6),

$$\frac{dm^*}{da} = \left(1 + U^2 - \frac{2m^*}{R}\right)^{1/2} \left(\frac{l^2}{R^2} + \mu^2 c^2\right)^{1/2} \frac{G}{c^3}, \quad (6')$$

which after integration yields

$$M_\infty c^2 = A(1 + U^2)^{1/2} c \left(\frac{l^2}{R^2} + \mu^2 c^2\right)^{1/2}$$

$$- \frac{1}{2} \frac{A^2}{R} c^2 \left(\frac{l^2}{R^2} + \mu^2 c^2\right) \frac{G}{c^4}. \quad (7')$$

Here again a quasi-Newtonian interpretation is possible. Whereas expression (5') constitutes the fourth physical component of  $p_\mu$  as seen by a comoving observer, the first term in the expression for  $M_\infty$  is that same component as seen by a freely falling observer at constant radius. The second term of  $M_\infty$  is again the gravitational energy of the hollow sphere. Here only the rest mass and the angular energy, but none of the radial motion, contribute to the source of the gravitational energy (see also Kuchař<sup>4</sup>).

The total mass energy is the energy integral for the radial motion of the whole collective ensemble.

It is evident from Eq. (7') that (a) Fig. 1 depicts the locus of turning points of the radial motion for ensembles characterized by various angular momenta, and that (b) for sufficiently high mass energy  $M_\infty$ , or low enough angular momentum  $l$ , a black hole, i.e., a completely collapsed configuration, is formed. Furthermore, an appropriate combination of mass energy and angular momentum will result in an unstable configuration, a "particle geon," balanced at the verge of collapse. In general, however, a geon

merely constitutes a temporary transition-state complex<sup>9</sup> of a collisionless particle ensemble imploding towards a black hole.

For massless particles, such as photons (or "gravitons"), Eq. (7) gives directly the geometrical-optics limits of the mass energy of electromagnetic<sup>10</sup> waves (or gravitational<sup>11</sup> waves) held together by their own gravitational field. Why do such geons give rise to a direct encounter with quantum geometrodynamics? Let us consider the dimensions of a geon with the smallest possible angular momentum. Rewrite Eq. (7), with  $\mu = 0$ , in dimensionless form; letting the angular momentum assume its quantum values,

$$l^2 = L(L + 1)\hbar^2,$$

and letting

$$\bar{n} = A^{1/2} [L(L + 1)]^{1/4}, \quad (10)$$

the mean "excitation number," i.e., the geometrical mean of the number of photon quanta and the number of angular momentum quanta, we have

$$\frac{M_\infty}{\bar{n} M_{PW}} = \frac{\bar{n} R_{PW}}{R} - \frac{1}{2} \left(\frac{\bar{n} R_{PW}}{R}\right)^3 \quad (11)$$

(see Fig. 3). Here  $M_{PW} = (\hbar c/G)^{1/2}$  and  $R_{PW} = (\hbar G/$

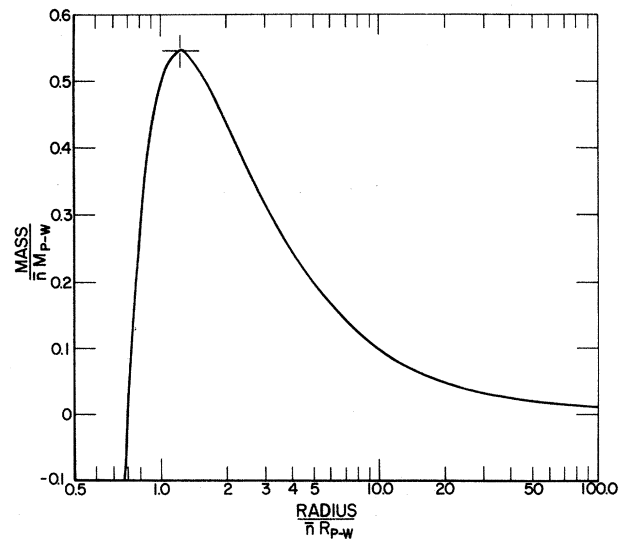


FIG. 3. Effective potential for collective motion of an electromagnetic (zero rest mass) geon. Vertical axis is the mass in units  $\bar{n} M_{PW}$ . Horizontal axis is the radius in units  $\bar{n} R_{PW}$ . In these units Eq. (11) reads  $y = 1/X - \frac{1}{2} X^3$ . It is evident therefore that the only equilibrium configuration (which is unstable) has a radius  $R = (9/8)$ (Schwarzschild radius), independent of the photon and the angular momentum number. It is the limiting configuration of the unstable branch in Fig. 2.

$c^3)^{1/2}$  are the Planck-Wheeler mass and length, respectively. It is evident that the total mass and the size of a geon depend on its mean excitation number, Eq. (10). In the limit of zero rest mass, a wave field characterized by a single quantum of angular momentum,  $L = 1$ , and a single photon (or graviton),  $A = 1$ , the size of the geon is

$$\bar{n}R_{PW} = 2^{1/4}R_{PW} = 2^{1/4} \times 1.616 \times 10^{-33} \text{ cm.}$$

This is precisely the dimension at which the fluctuations in the geometry<sup>12</sup> become appreciable, i.e., where classical theory becomes inapplicable, and quantum geometrodynamics must enter. Here one should mention parenthetically that the spherical approximation will also become inapplicable because single-photon or -graviton fields are not spherically symmetric.

The author appreciates the hospitality of Battelle Memorial Institute.

---

\*Present address: Mathematics Department, Ohio State University, Columbus, Ohio 43210.

<sup>1</sup>For a review see C. W. Misner in *Brandeis Summer Institute 1966 Lectures in Theoretical Physics: Astrophysics and General Relativity*, edited by M. Chretien, S. Deser, and J. Goldstein (Gordon and Breach, New York, 1968).

<sup>2</sup>M. M. May and R. H. White, *Phys. Rev.* **141**, 1232

(1966).

<sup>3</sup>J. Oppenheimer and H. Snyder, *Phys. Rev.* **56**, 455 (1939), first analyzed homogeneous, pressureless collapse. For nonzero pressure the analysis was done by H. Bondi, *Nature* **215**, 838 (1967), and *Mon. Notic. Roy. Astron. Soc.* **142**, 333 (1969); see also W. B. Bonnor and M. C. Faulkes, *ibid.* **137**, 239 (1967).

<sup>4</sup>K. Kuchar, *Czech. J. Phys.* **B18**, 435 (1968), has done an analysis of thin-shell dynamics for matter obeying an adiabatic equation of state. See also J. E. Chase, *Nuovo Cimento* **B67**, 136 (1970).

<sup>5</sup>J. L. Synge, *The Relativistic Gas* (Interscience, New York, 1957).

<sup>6</sup>Unstarred masses (such as  $m, M$ ) are in conventional units, starred masses are in geometrical units; e.g.,  $m^* = mG/c^2$  (cm).

<sup>7</sup>Our variational principle is modeled after the one found in B. K. Harrison, K. S. Thorne, M. Wakano, and J. A. Wheeler, *Gravitation Theory and Gravitational Collapse* (Univ. of Chicago, Chicago, Ill., 1965).

<sup>8</sup>C. W. Misner and D. H. Sharp, *Phys. Rev.* **136**, B572 (1964).

<sup>9</sup>R. Ruffini and J. A. Wheeler, to be published. For a summary see R. Ruffini and J. A. Wheeler, *Bull. Amer. Phys. Soc.* **15**, 76 (1970).

<sup>10</sup>J. A. Wheeler, *Geometrodynamics* (Academic, New York, 1962), Chap. 2.

<sup>11</sup>D. R. Brill and J. B. Hartle, *Phys. Rev.* **135**, B271 (1964).

<sup>12</sup>This fact has been already observed by Wheeler in Ref. 10. See also J. A. Wheeler, in *Relativity, Groups, and Topology*, edited by C. DeWitt and B. DeWitt (Gordon and Breach, New York, 1964), p. 327.

---

## Form-Factor Ratio $G_E(n)/G_E(p)$ at Low Momentum Transfers\*

F. A. Bumiller, F. R. Buskirk, and J. W. Stewart†

*Department of Physics, Naval Postgraduate School, Monterey, California 93940*

and

E. B. Dally‡

*Stanford Linear Accelerator Center, Stanford University, Stanford, California 94305*

(Received 15 July 1970)

Measurements of the ratio of the deuteron to proton electric form factors,  $G_E(d)/G_E(p)$ , were made from elastic electron-deuteron scattering to a precision of approximately 1% for the range of momentum transfers  $0.10 \leq q^2 \leq 0.8 \text{ F}^{-2}$ . Within experimental errors the slope as obtained from the ratio  $G_E(n)/G_E(p)$  agrees with the extrapolated thermal neutron-electron interaction slope when relativistic corrections and Feshbach-Lomon deuteron wave functions are applied. The deuteron radius was found to be  $1.95 \pm 0.02 \text{ F}$ , the same as predicted by the Feshbach-Lomon calculation.

We have measured the ratio of elastic electron-deuteron scattering to elastic electron-proton scattering in the range of momentum transfers  $0.1 \leq q^2 \leq 0.8 \text{ F}^{-2}$  with a precision of 1% or better. It is possible to extract from such measurements

values for the ratio  $G_E(n)/G_E(p)$ .<sup>1</sup> We report this ratio and apply the best known fits of  $G_E(p)$  to extract a value of  $G_E(n)$ .

There has been a discrepancy between the slope of the neutron-electron interaction mea-